Magnetic, heat capacity, and conductivity studies of ferrimagnetic $MnCr_2S_4$ single crystals

V. Tsurkan,[1,2] M. Mücksch,[1] V. Fritsch,[1] J. Hemberger,[1] M. Klemm,[1] S. Klimm,[1] S. Körner,[1] H.-A. Krug von Nidda,[1] D. Samusi,[2] E.-W. Scheidt,[1] A. Loidl,[1] S. Horn,[1] and R. Tidecks[1]

[1]*Institut für Physik, Universität Augsburg, Universitätsstraße 1, D-86159 Augsburg, Germany*

[2]*Institute of Applied Physics, Academy of Sciences of Moldova, str. Academiei 5, MD 2028, Chisinau, Republic of Moldova*

(Received 7 January 2003; published 21 October 2003)

Magnetization, ferromagnetic resonance (FMR), heat capacity, and electrical conductivity of $MnCr_2S_4$ spinel single crystals were investigated as a function of temperature and magnetic field. Two λ anomalies observed in the heat capacity correlate with magnetic phase transformations and their field dependence found in magnetization measurements. The upper λ anomaly at a temperature of ~65 K marks the onset of ferrimagnetic ordering, while the lower one at ~4.8 K indicates an additional antiferromagnetic ordering of the A(Mn) sublattice. Below the Curie temperature, magnetization, and FMR measurements revealed a positive magnetocrystalline anisotropy. The dominating role of the B(Cr) sublattice in generating this anisotropy is shown.

DOI: 10.1103/PhysRevB.68.134434 PACS number(s): 75.50.Pp, 75.50.Gg, 76.50.+g, 65.40.Ba

I. INTRODUCTION

Recent reports on the colossal magnetoresistance[1] (CMR) and half-metallic (HM) ferromagnetic properties[2] of the semiconductor $FeCr_2S_4$ have renewed the interest in magnetic ternary chalcogenides. Among this group of materials, $MnCr_2S_4$ is of particular importance for designing HM antiferromagnets, which may, e.g., be used for spin-polarized scanning tunneling microscopy.[3] $MnCr_2S_4$ crystallizes in a normal spinel structure (space group $Fd3m$), in which Mn and Cr ions occupy tetrahedral A and octahedral B sites, respectively. It exhibits a complicated magnetic behavior in the ferrimagnetic state, which evolves at low temperatures.[4,5]

Contradictory data were published previously on the magnetic properties of polycrystalline $MnCr_2S_4$. The Curie temperature of nominally stoichiometric samples varies from 66 K to 95 K.[4–6] Neutron-diffraction experiments on polycrystalline $MnCr_2S_4$ yield a magnetic moment of $3\mu_B$ for the chromium ion in accordance with a $3d^3$ state.[6] But the measured magnetic moment of $4.7\mu_B$ for the manganese ions deviates from $5\ \mu_B$ expected for a $3d^5$ configuration. This indicates a deviation from the pure S state of the Mn ion according to Ref. 6. Recent x-ray photoelectron-spectroscopy studies of $MnCr_2S_4$ single crystals[7] were interpreted in terms of a local moment of Cr^{3+} ions close to $3\mu_B$ in agreement with the neutron-diffraction data. A reduced splitting of the $3s$ core-level spectra of the Mn^{2+} ion as compared to that of manganese oxides was obtained and attributed to an increase in covalency.[7]

Based on the saturation behavior of the magnetization observed in magnetic fields above 20 kOe and on the absence of a (200) peak in the neutron-diffraction pattern at 4.2 K, a collinear arrangement of the magnetic moments of Mn and Cr ions was suggested.[6] But from other magnetization[5,8–10] and neutron-diffraction[11] investigations a change of the magnetic structure below 5.5 K was inferred. This change was interpreted as a first-order phase transition from a collinear Néel-type structure[12] with antiparallel alignment of the magnetic moments of the Mn and Cr sublattices to the Yafet-Kittel-type two-dimensional noncollinear structure[13] with a canted spin structure of the Mn ions. The canting was assigned to strong antiferromagnetic A-A interactions. For magnetic fields larger than 100 kOe a more complicated three-dimensional spin configuration was proposed.[14,15] It was shown that higher order contributions to the exchange interactions, especially biquadratic A-A exchange, are important for the realization of this spin structure.[14–17] However, the framework of the interactions considered was not sufficient to completely explain the magnetic structure of $MnCr_2S_4$. This suggests the presence of additional, e.g., anisotropic interactions. Recently, a strong magnetocrystalline anisotropy has indeed been found in $MnCr_2S_4$ single crystals.[18] The anisotropy field ($H_A = 2K_1/M_s$, where K_1 is the first anisotropy constant and M_s the spontaneous magnetization) reaches a value of about 1 kOe at 4.2 K, unexpectedly large for octahedrally coordinated Cr^{3+} ions with a quenched orbital moment, or tetrahedrally coordinated Mn^{2+} ions in a pure S state.

To clarify the origin of the above described discrepancies in the magnetic data published on polycrystalline samples and to reveal the intrinsic properties of this compound we performed detailed magnetization, ferromagnetic resonance (FMR), heat capacity, and conductivity studies of $MnCr_2S_4$ single crystals.

II. EXPERIMENTAL TECHNIQUES

$MnCr_2S_4$ single crystals were grown by the chemical transport-reaction method[19] from the ternary polycrystalline material prepared by solid-state reactions. Chromium chlorine was used as a transport agent. X-ray diffraction analysis confirmed the single-phase spinel structure of powdered single-crystalline samples. The lattice parameters, a_0, for single crystals from different batches varied from 10.116(2) Å to 10.119(2) Å, and are within the range reported for polycrystalline samples (10.107–10.129 Å).[4,20,21] In addition, the sample composition was checked by (EDX) analysis. Within the accuracy of this method (~5% for cations and ~10% for sulfur) no deviations from the nominal stoichiometry was found for single-crystalline samples from different batches.

Quantum Design MPMS-7 and MPMS-5 SQUID magne-

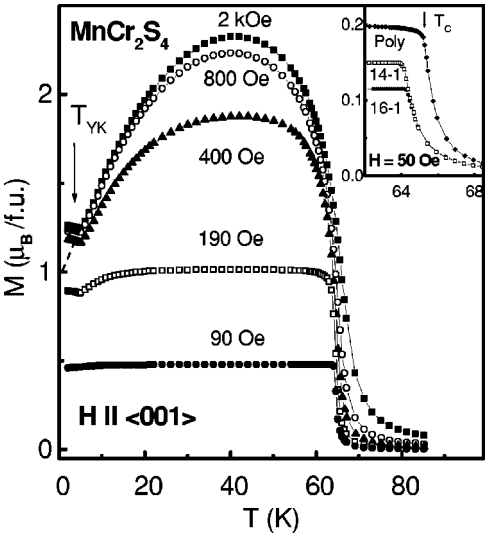

FIG. 1. Temperature dependence of the magnetization, M, in Bohr magneton μ_B per formula unit, in different magnetic fields applied in the $\langle 001 \rangle$ direction for a $MnCr_2S_4$ single crystal (sample 16-13). Inset: Magnetization in the region of the paraferrimagnetic transition for samples 16-1, 14-1, and the polycrystal 7-8 in a field of 50 Oe. Arrows indicate the temperatures of the magnetization anomalies at the Curie temperature, T_C, and at T_{YK} (see the text). Solid lines are guides to the eye.

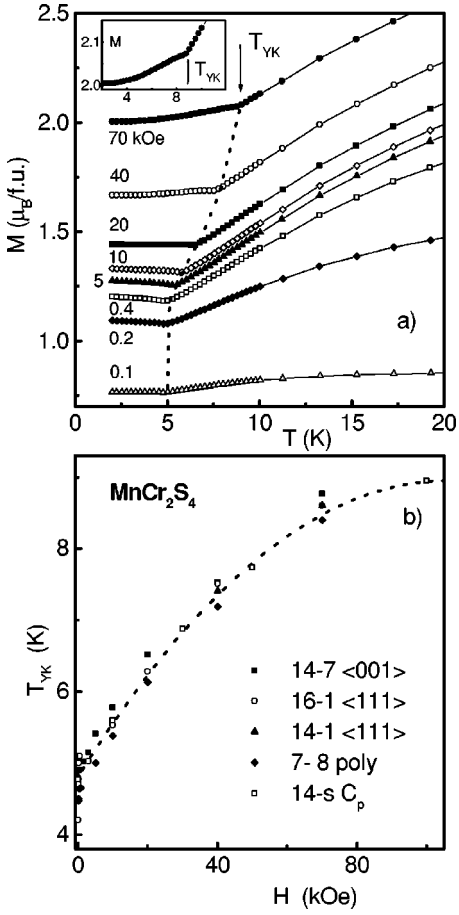

FIG. 2. (a) Temperature dependences of the magnetization in different magnetic fields applied in the $\langle 001 \rangle$ direction for a $MnCr_2S_4$ single crystal (sample 14-7) in the temperature range below 20 K. Inset: $M(T)$ for a field of 70 kOe. (b) Field dependence of the temperature T_{YK} of the anomaly in magnetization and heat capacity for different samples. Solid and dotted lines are guides to the eye.

tometers operating in the temperature range $2\,K < T < 400\,K$ and magnetic fields up to 70 kOe were used for static magnetization measurements. Ferromagnetic resonance studies were performed in a cw X-band spectrometer (Bruker ELEXSYS E500) equipped with a continuous He gas-flow cryostat (Oxford Instruments) working in the temperature range $4.2\,K < T < 300\,K$. The heat capacity was studied by τ relaxation and adiabatic methods[22,23] in the temperature range $1.5\,K < T < 20\,K$ and by an ac method[24] for temperatures $7\,K < T < 200\,K$ in magnetic fields up to 100 kOe. For conductivity studies a dc two-probe method was used owing to the high sample resistivity (of order of $10^{12}\ \Omega$ at room temperature). Resistivity measurements in the temperature range from 350 K down to 90 K were performed using a commercial cryostat (Oxford Instruments). Below 90 K the resistivity exceeds the limit of the electrometer.

III. EXPERIMENTAL RESULTS

A. Magnetization

Figure 1 presents the temperature dependences of the magnetization for one of the single-crystalline samples in various magnetic fields below 2.5 kOe. The field was applied in the $\langle 001 \rangle$ direction. For temperatures below 65 K and fields lower than 100 Oe the Curie temperature T_C is marked by a kink in the magnetization. In the range $30\,K < T < T_C$, a nearly temperature independent plateau develops, due to demagnetization effects.[25] The value of T_C is found to be (64.3 ± 0.2) K for samples from different batches. This is by about 1 K lower than for polycrystalline $MnCr_2S_4$ (see inset in Fig. 1). The demagnetizing field is of the order of the magnetization and depends on the shape of the sample, resulting in a shape-dependent magnetization for low fields, for which the sample is in a multidomain state. For high fields, the sample is in a single-domain state. Here the magnetization shows a nonmonotonic temperature dependence below T_C with a maximum at around 42 K. For low temperatures the magnetization approaches a value of $1\,\mu_B$ (dashed line in Fig. 1), which corresponds to the expected resulting magnetic moment, if the moments of the Cr and Mn ions are assumed to be in an antiparallel collinear arrangement. However, below 5 K the magnetization levels of to a nearly constant value (about $1.23\,\mu_B$) down to the lowest temperature measured (1.8 K).

In Fig. 2(a) the temperature dependence of the magnetization in the temperature range $1.8\,K < T < 20\,K$ is presented for magnetic fields up to 70 kOe. The behavior of the magnetization is similar to that observed earlier in polycrystalline samples of $MnCr_2S_4$ in fields up to 30 kOe. A change of the slope of $M(T)$ is attributed to a transition from a collinear to a noncollinear magnetic structure of the Yafet-Kittel type. The associated transition temperature is determined to be $T_{YK} \sim 5.5\,K$.[5] The transition temperature T_{YK} of our single

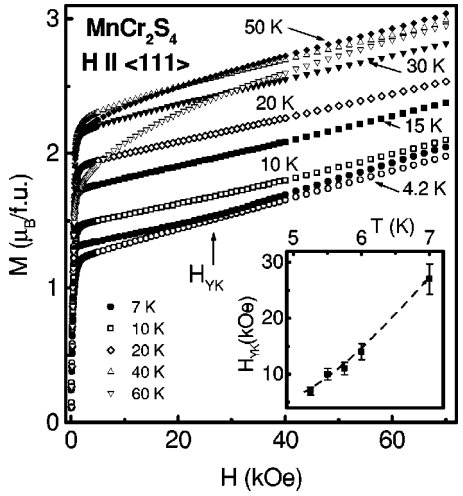

FIG. 3. Field dependence of the magnetization at different temperatures for a $MnCr_2S_4$ single crystal (sample 14-5). The field H is applied in the $\langle 111\rangle$ direction. Inset: Temperature dependence of the field corresponding to the change of the slope of the magnetization curve for $5\ \mathrm{K}<T<7\ \mathrm{K}$. Solid lines are guides to the eye.

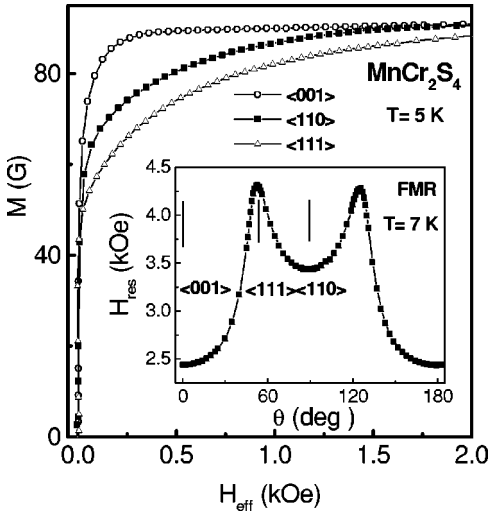

FIG. 4. Magnetization versus internal magnetic field $H_{\mathrm{eff}}=H-NM$ (here N is the demagnetizing coefficient, determined from the $M(T)$ curves in low fields close to T_{C}) for different crystallographic directions in a $MnCr_2S_4$ single crystal (sample 16-13) at 5 K. Inset: Angular dependence of the ferromagnetic resonance field for a disklike single-crystalline $MnCr_2S_4$ sample (16-13d3) within the (110) plane at 7 K. Solid lines are guides to the eye.

crystals varies slightly for samples from different batches. It does not depend on the orientation of the magnetic field with respect to the crystallographic axes [see Fig. 2(b)]. Data taken from our poly- and single-crystalline samples are in excellent agreement [also presented in Fig. 2(b)]. The observed field dependence of the characteristic temperature, T_{YK} [Fig. 2(a)], is nearly two times weaker than reported previously for polycrystalline samples[14,26] and, in contrast to earlier results, shows a saturation in high magnetic fields. In addition to the abrupt change of slope at T_{YK}, the $M(T)$ curves for the highest fields exhibit another less pronounced one before a plateau for temperatures below 4 K, as shown in the inset in Fig. 2(a).

Figure 3 shows the magnetization versus field for several temperatures below T_{C}. The most striking features of the magnetization curves are the steep slope in high fields and the absence of a saturation for all temperatures below T_{C}, including $T<T_{\mathrm{YK}}$. For temperatures above 5 K, the magnetization changes slope at a characteristic field H_{YK}. Below 7 K the characteristic field H_{YK} increases with increasing temperature (see the inset in Fig. 3). A similar behavior was observed previously on polycrystalline samples and was attributed to the transition from the collinear to the noncollinear structure.[9,10] Above 8 K, the transition from the low-field to high-field magnetic structure is considerably broadened and does not allow us to determine the transition temperature accurately. This may explain the difference between our and earlier data concerning the field dependence of T_{YK}.

Another important finding is a pronounced dependence of the magnetization on the crystallographic direction, i.e., the magnetocrystalline anisotropy (Fig. 4). Below the Curie temperature, the easy axis of magnetization is the $\langle 001\rangle$ direction, while the $\langle 110\rangle$ and $\langle 111\rangle$ directions correspond to the intermediate and hard axes, respectively. The presence of a strong magnetocrystalline anisotropy was confirmed by recent ferromagnetic resonance studies presented in detail in Ref. 18. A typical angular dependence of the resonance field is shown in the inset of Fig. 4. Here the static magnetic field is applied within the (110) plane of a disk-shaped single crystal. The resonance field exhibits a maximum in the $\langle 111\rangle$ and a minimum in the $\langle 001\rangle$ directions, respectively. This is a characteristic for a positive cubic magnetocrystalline anisotropy.[27]

The values of the first (K_1) and second (K_2) anisotropy constants, as calculated from the angular dependences of the resonance field at 7 K, are approximately 4.2×10^4 and 10^5 erg/cm^3, respectively.[18] Both constants increase monotonously with decreasing temperature. Figure 5(a) presents the temperature dependence of the first anisotropy constant K_1 normalized to its value at 7 K.[28] In this figure we also plotted the temperature dependences of the spontaneous magnetization in M_s[10] representation for the Cr and Mn sublattices, normalized to their values at 4 K. To obtain the values of the spontaneous magnetization of the sublattices, the magnetization of $CdCr_2S_4$ was measured and then its spontaneous part was subtracted from the net spontaneous magnetization of $MnCr_2S_4$. Results are shown in Fig. 5(b). For the above procedure to yield the correct result, the Cr sublattice has to show similar behavior in both compounds. The assumption of such a similar behavior is based on the following facts. The two compounds are isostructural and the lattice constant of ferromagnetic $CdCr_2S_4$ (10.23 Å) is close to that of $MnCr_2S_4$.[21] The Curie temperature of $CdCr_2S_4$, $T_{\mathrm{C}}=84.5$ K, is also close that of $MnCr_2S_4$. In both compounds the exchange interactions in the B sublattice mainly dominate their magnetic properties.[5] The interactions depend on the electronic configuration of the B ions, i.e., Cr^{3+} ($3d^3$) with a half filled t_{2g} level, and their mutual nearest neighbor distance. In the chromium oxide spinels the dominant interaction is the direct antiferromagnetic Cr-Cr-exchange, for ex-

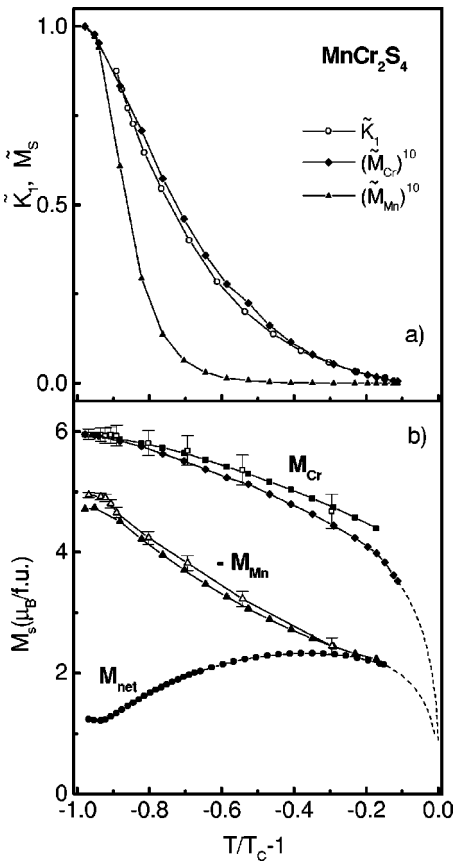

FIG. 5. (a) Temperature dependences of the normalized first anisotropy constant $\tilde{K}_1 = K_1(T)/K_1(7\,\mathrm{K})$ and the tenth power of the spontaneous magnetization $\tilde{M}_s = [M_s(T)/M_s(4\,\mathrm{K})]^{10}$ of the Cr and Mn sublattices. (b) Temperature dependences of the macroscopic (closed symbols) and local (open symbols) magnetic moments of the Cr and Mn sublattices, obtained from the magnetization data (present paper) and neutron-diffraction data (Ref. 17). Closed squares and diamonds represent the data obtained by extrapolations of $M(H)$ curves from fields above 30 kOe and below 10 kOe, respectively. Solid and dotted lines are guides to the eye.

ample as in $ZnCr_2O_4$,[29] while in the chromium sulfide spinels, where the Cr-Cr distance is larger due to the larger radius of the sulfur ions as compared to the oxygen ions, the ferromagnetic superexchange via the sulfur ions is more important.[30]

All values of the spontaneous magnetization were obtained from the extrapolation of the $M(H)$ curves to $H \rightarrow 0$. The spontaneous magnetization of Cr was determined in two ways: by extrapolation of the high field data above 30 kOe, used for comparison with the local magnetic moment, and by extrapolation of the data below 10 kOe for comparison with the anisotropy constant, determined by the ferromagnetic resonance in fields below 10 kOe as well. The spontaneous magnetization of the Cr sublattice, which exhibits an experimental value of $(5.8 \pm 0.05)\mu_B$ at $T = 4$ K, was adjusted to the low temperature value of $5.95\mu_B$ obtained by neutron diffraction.[17] The spontaneous magnetization of the Cr ions of $CdCr_2S_4$ single crystals correlates well with the local moment of the Cr sublattice of $MnCr_2S_4$ measured by neutron diffraction [see Fig. 5(b)]. This further justifies the assumption used above. The temperature dependence of the Cr-sublattice magnetization is typical for a ferromagnet below T_C. The data near T_C shown by dashed lines are not used for the evaluation because of the large uncertainty in the high-field extrapolation procedure on approaching the critical region.

The results of the calculations of the Mn-sublattice magnetization, obtained from the high-field extrapolation, are also shown in Fig. 5(b). We note that our calculations correlate well with the temperature dependence of the local magnetic moments of the Mn ions obtained by neutron diffraction.[17] For the Mn sublattice a Curie-Weiss-like change is seen in the range $0.1 < T/T_C < 0.8$, probably indicating a nonsaturated state. The fact that all calculated values are located below the neutron diffraction data may be connected to the canting of the Mn moments with respect to the Cr moments. This effect increases at temperatures below T_{YK}.

An additional important result presented in Fig. 5(a) is related to the rather good scaling of the temperature dependence of the first anisotropy constant K_1 with the tenth power law of the normalized saturation magnetization $[M_s(T)/M_s(4\,\mathrm{K})]^{10}$ of the Cr sublattice, obtained by extrapolation from the fields below 10 kOe, as expected from a single ion model.[27] In contrast, the $K_1(T)$ dependence strongly differs from that of $[M_s/M_s(4\,\mathrm{K})]^{10}$ for the Mn sublattice.

B. Heat capacity

In Fig. 6(a) the molar heat capacity, C_p, divided by T, of a $MnCr_2S_4$ single crystal is plotted versus a logarithmic temperature scale for $H = 0$ and $H = 100$ kOe. Two pronounced λ-type anomalies are observed, which correlate with the magnetic phase transitions shown in Fig. 6(b).

The onset of magnetic order at T_C is signaled by the λ anomaly at high temperatures. A strong magnetic field suppresses this anomaly considerably, yielding a broadening of the transition and a shift to higher temperatures. This behavior is characteristic for a ferromagnetic transition (see, e.g., Refs. 31 and 32).

The low-temperature anomaly of the heat capacity in zero field perfectly coincides with the low-temperature magnetization anomaly at T_{YK}. No noticeable hysteresis is found in the heat-capacity data for this phase transition. An applied magnetic field shifts the λ anomaly to higher temperatures. However, even at 100 kOe the anomaly remains well defined, in contrast to the anomaly at T_C.

The evolution of C_p under an applied magnetic field is shown in Fig. 7. The field dependence of T_{YK} as observed in the heat capacity measurements coincides with that determined for the low-temperature magnetization anomaly and has already been included in Fig. 2(b). In nonmetallic ferrimagnets the specific heat is expected to vary as $C_p = \beta T^3 + \delta T^{3/2}$ for temperatures much lower than the Debye temperature Θ_D. The first term represents the contribution of the lattice and the second one that of the spin waves.[33] Therefore, a plot $C_p T^{-3/2} = f(T^{3/2})$ should reveal a straight line

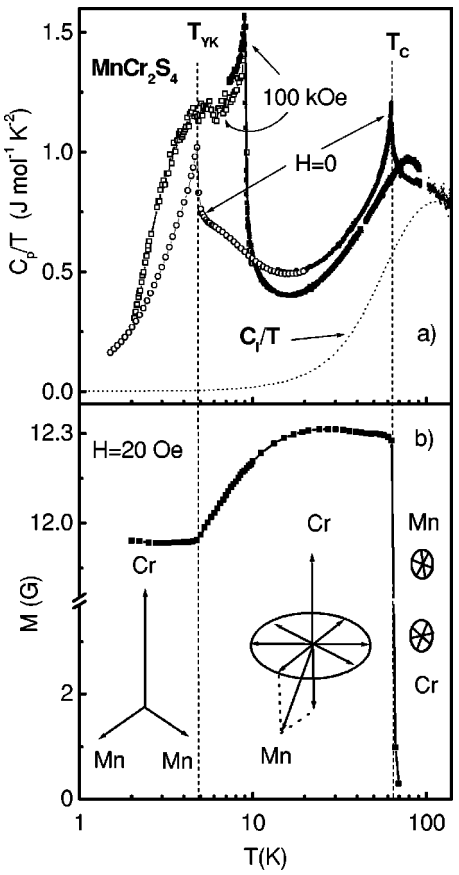

FIG. 6. (a) Temperature dependence of the molar heat capacity, C_p, divided by the temperature T for a $MnCr_2S_4$ single crystal (sample 14-s) measured by τ relaxation (open circles), adiabatic (open squares), and ac (closed symbols) methods, respectively, for zero and 100 kOe. Dotted line shows the lattice contribution. (b) Temperature dependence of the magnetization of the same sample measured in low field. Dashed lines indicate the temperatures T_C and T_{YK}. The proposed magnetic structure is indicated schematically. Solid lines are guides to the eye.

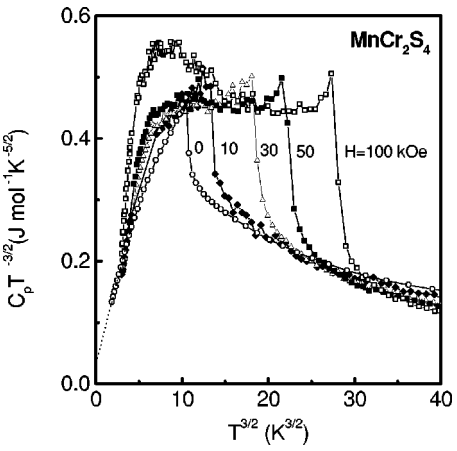

FIG. 7. Molar heat capacity $C_pT^{-3/2}$ vs. $T^{3/2}$ at different magnetic fields for a $MnCr_2S_4$ single crystal (sample 14-s). The dotted line shows the linear fit to the low temperature data for the zero field curve. Solid lines are guides to the eye.

with slope β and intercept δ. Such a behavior was found in a number of ferrimagnets (see, e.g., Refs. 34–37). However, for $MnCr_2S_4$, a fit to the lower temperature part (1.5 K–2.3 K) of the data for zero field (dotted line in Fig. 7) gives an unrealistic value of about 33 K for the Debye temperature Θ_D, calculated using the standard expression for the coefficient $\beta = 12\pi^4 n N_A k_B / 5\Theta_D$.[3] Here n is the number of atoms per formula unit, N_A is Avogadro's number, and k_B is the Boltzmann constant. Similarly, the value of δ is more than two orders of magnitude higher than that observed in the referred ferrimagnets.[34–37]

For the whole temperature range the lattice contribution to the specific heat, C_l [dotted line in Fig. 6(a)] was calculated numerically using a Debye model. The lattice contribution was adjusted to the high-temperature part ($T > 100$ K) of the experimental data, since the critical spin fluctuations can be neglected at high temperatures, as was shown for $MnCr_2S_4$ polycrystals.[38] From this simulation a Debye temperature of about 410 ± 30 K was estimated. This value is compared well to the typical Debye temperature (~ 600 K) in oxide spinels,[37] if one take into account the higher mass and the weaker bonding in thiospinels compared to oxyspinels. The lattice contribution to the specific heat at temperatures below 10 K does not exceed 5% of the overall value of C_p. Conductivity studies of our single crystals (see Sec. III C) suggest a very low number of charge carriers and, therefore, a negligible electronic contribution to C_p. Thus, the variation of the heat capacity C_p below 10 K appears to originate mainly from magnetic degrees of freedom.

In Fig. 8(a) we plotted the temperature dependent molar entropy, S_m, associated with the magnetic degrees of freedom, inferred from the magnetic heat capacity $C_m = C_p - C_l$ by integration. Using $S_m = R \ln(2S+1)$, and taking into account both Mn and Cr ions, the entropy in the paramagnetic state must correspond to $2R \ln 4 + R \ln 6$ per mole of $MnCr_2S_4$. Here we assume Cr^{3+} ions with $S = 3/2$ and Mn^{2+} ions with $S = 5/2$. However, only 77% of this value is reached at the Curie temperature T_C. This indicates a reduction of the magnetic entropy already in the paramagnetic region due to critical fluctuations. An external magnetic field results in a further reduction, which supports the interpretation of a short-range order above T_C [see Fig. 8(a)]. At temperatures above $2T_C$ the magnetic entropy approaches the expected theoretical limit and hence justifies our assumption concerning the lattice contribution.

The application of a magnetic field yields a considerable increase of the entropy at low temperatures [Fig. 8(b)]. As can be inferred from Fig. 5(b), the Cr sublattice is nearly completely ordered below 12 K. Therefore, entropy changes below this temperature can mainly be attributed to the dynamics of the ordering of the Mn sublattice. In zero field, the entropy at the transition temperature T_{YK} reaches only about 12% of the expected $R \ln 6$ for the complete disorder in the Mn sublattice, whereas in a field of 100 kOe, $S_m(T_{YK})$ increases up to 52% of the expected value [see inset in Fig. 8(b)]. This indicates an increasing disorder of the Mn sublattice at $T = T_{YK}$ with increasing field.

For temperatures below 15 K, the C_p/T curve for zero field in Fig. 6(a) shows an increase with decreasing tempera-

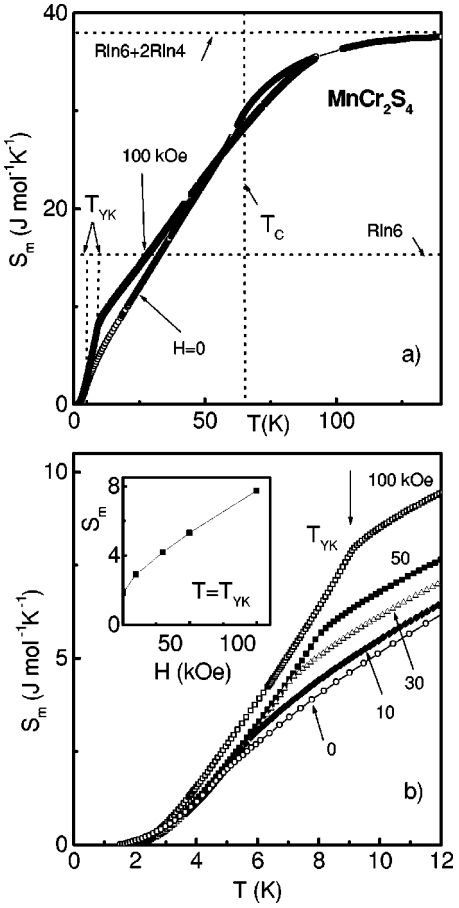

FIG. 8. Temperature dependence of the magnetic entropy S_m at different magnetic fields: (a) for the temperature range 1.5 K$<T<$140 K. Horizontal dotted lines indicate the values $R\ln 6$ and $R\ln 6+2R\ln 4$. Vertical dotted lines mark the temperature of transitions at T_C and T_{YK}. (b) low-temperature behavior. Inset: Field dependence of the magnetic entropy reached at the transition temperature T_{YK}. Solid lines are guides to the eye.

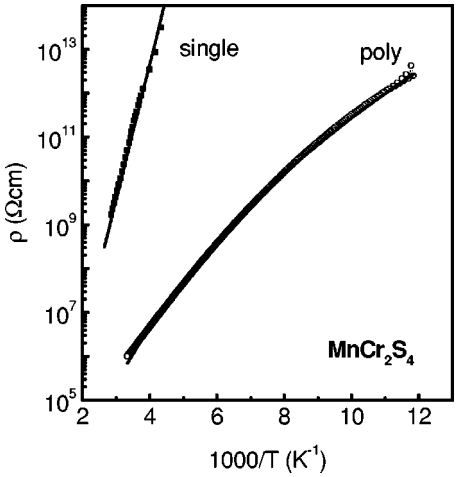

FIG. 9. Temperature dependence of the resistivity of $MnCr_2S_4$ polycrystals (sample 7-8) and single crystals (sample 16-R) plotted in a semilogarithmic scale versus the inverse temperature. Solid lines present fits by the Arrhenius and variable-range-hopping (VRH) law to the experimental data for the single- and polycrystalline samples, respectively.

ture due to an additional broad anomaly on which the λ anomaly at 5 K seems to be superimposed. For high fields this additional anomaly is clearly separated from the λ anomaly at T_{YK} [see, Figs. 6(a) and 7] and becomes more pronounced. It seems to be correlated to the magnetization changes below T_{YK}, as shown in the inset of Fig. 2(a).

C. Resistivity

In Fig. 9 the temperature dependence of the resistivity for poly- and single-crystalline $MnCr_2S_4$ samples is shown. In the temperature range 230–350 K, the resistivity of the single crystals strongly decreases with increasing temperature. The resistivity data follow a simple Arrhenius law $\rho=\rho_0\exp(\Delta E/k_BT)$ with an activation energy ΔE of about 0.6 eV.

In comparison, the resistivity of polycrystals measured in the temperature range 70–300 K is about four orders of magnitude lower. The Arrhenius law describes only the high-temperature part of the $\rho(T)$ curve, yielding an activation energy nearly three times smaller (about 0.2 eV) than that of single crystals. We attribute this difference in the activation energies to a contribution of impurity-induced conduction in the polycrystalline sample, while the single crystal probably reflects the intrinsic gap of this compound. The low-temperature data for the resistivity of the polycrystalline sample can be described rather with Mott's variable-range-hopping (VRH) model $\rho=\rho_0\exp(T_0/T)^{1/4}$. This suggests that charge transport takes place by VRH similar to the case of CMR perovskite manganites at $T>T_C$.[39–41] Although a charge compensation due to the possible presence of cation and anion vacancies cannot be excluded, the pronounced insulating behavior observed for single-crystalline $MnCr_2S_4$ samples most probably indicates a rather low concentration of charge carriers.

IV. DISCUSSION

Summarizing the experimental findings given above, the anomalies exhibited by the specific heat and the magnetization of $MnCr_2S_4$, can be attributed to a common origin. Starting at high temperatures, the λ anomaly in the specific heat at $T_C\approx 65$ K, indicates the onset of magnetic order. Below T_C, the magnetization increases as in a ferromagnet down to 42 K. The increase is mainly caused by the ordering of the Cr sublattice (see Fig. 5). Cooling below 42 K, the magnetization decreases again, due to an antiferromagnetic aligning of the Mn with respect to the Cr sublattice (Fig. 5). This decrease of the magnetization corresponds a broad peak in C_p/T with a maximum at around 5 K. In addition, the specific heat shows another λ anomaly at $T_{YK}\approx 4.8$ K. At this temperature the magnetization exhibits a distinct kink and changes only weakly for $T<T_{YK}$. In an external magnetic field, both λ anomalies are shifted to higher temperatures: the λ anomaly at T_C broadens, whereas the anomaly at T_{YK} remains sharp. In contrast, the maximum of the broad anomaly in C_p/T remains near 5 K but the weight is redis-

tributed with increasing field from the high-temperature to the low-temperature wing.

Based on these findings, we suggest the following scenario of magnetic ordering in $MnCr_2S_4$. At T_C the Cr sublattice orders ferromagnetically, whereas the Mn sublattice still remains quasiparamagnetic. In the quasiparamagnetic state the longitudinal component of the magnetic moment of the Mn sublattice is ordered antiparallel to the moment of the Cr sublattice, whereas the transverse component of the moment of the Mn sublattice is fully disordered. On decreasing temperature the Mn ions gradually align in the exchange field of the Cr sublattice with an effective antiferromagnetic orientation with respect to the Cr magnetization. This reduces the net magnetization and results in the broad low-temperature peak in C_p/T. Finally, at T_{YK} the onset of a canted antiferromagnetic order (of the transverse component of the moment of the Mn sublattice) within the Mn sublattice results in an effective triangular or more complicated structure. In the following we give the experimental evidence and discuss it in the light of corresponding results in the literature.

The transition at $T_C \approx 65$ K is an order-disorder phase transition between a ferrimagnetic and a paramagnetic state. A detailed analysis of the critical exponents that describe the thermodynamical behavior of magnetization and susceptibility of $MnCr_2S_4$ in the asymptotical temperature range has shown that this transformation is of second-order type.[38] An analysis of the behavior of the heat capacity singularity observed in the critical region is outside the scope of the present paper and will be presented elsewhere.

In the temperature range $T_{YK} < T < T_C$ the Cr sublattice, or the B-B interaction, is mainly responsible for the long-range magnetic properties of $MnCr_2S_4$. This we conclude from the fact that the ferrimagnetic state can be destroyed completely by a substitution of only $\sim 12\%$ of Cr by nonmagnetic In ions.[42] Substitutions on the Mn site does not affect the ferrimagnetism.[21] This conclusion is supported by similar results obtained by a substitution on the Cr sublattice in the isomorphous $CdCr_2S_4$ ferromagnet,[43] which contains only one type of magnetic ions on the B places. In that case the percolation threshold for the suppression of ferromagnetic order is also about 10%. Since the A-B interaction in $MnCr_2S_4$ is much weaker than the B-B interaction (see Refs. 5, 6), the antiferromagnetic arrangement of the Mn and Cr ions may be easily influenced by a magnetic field, yielding a strong increase of the magnetization in high fields.

The observed decrease of the net magnetization below 42 K can be ascribed to the quasiparamagnetic behavior of the Mn ions in the exchange field of the Cr sublattice. Our results demonstrate that the entropy change, associated with this effect, is shifted to low temperatures with increasing magnetic field [see Figs. 6(a) and 8(b)] yielding the broad anomaly in C_p/T. In addition, the net magnetization increases with increasing field, showing that the Cr moments become less compensated. This effect can probably be ascribed to a compensation of the exchange field of the Cr ions acting on the Mn sublattice by the external magnetic field, which results in a reduced antiferromagnetically alignment of the Mn ions with respect to the Cr ions.

The nature of the magnetic transformation at $T \sim 5$ K is apparently more complex. Attributing the magnetic and heat-capacity anomalies at T_{YK} to the transition from a collinear Néel magnetic structure to a triangular Yafet-Kittel-type configuration as suggested previously (see Ref. 5), we note the following. The absence of any hysteretic behavior of the heat capacity at T_{YK} seems to disagree with the proposed first-order type of this transition (Ref. 11). Moreover, the steep slope of the magnetization curves, observed in high fields, indicates that a noncollinear structure is realized at all temperatures. We suggest a second-order transition from a quasiparamagnetic into an antiferromagnetic state of the Mn sublattice due to the A-A interactions, with correlated transverse components of the magnetic moments of the Mn ions. This results in a canted antiferromagnetic magnetization of the Mn ions due to the influence of the Cr sublattice, or A-B interactions.

The possibility of an additional antiferromagnetic ordering of the Mn sublattice in $MnCr_2S_4$ crystals is in general agreement with the antiferromagnetic arrangement of the Mn ions observed in the related sulfide spinel $MnIn_2S_4$ [$T_N = 4.9$ K (Ref. 44)]. An antiferromagnetic ordering also occurs in the oxide spinel $MnGa_2O_4$. It is realized at much higher temperature[45] ($T_N = 33$ K) because of a stronger A-A interaction in the oxide compared to the sulfide compound. It is noteworthy here that in the case of $MnGa_2O_4$, the antiferromagnetic ordering is accompanied by an appearance of a (200) reflection in the neutron-diffraction pattern similar to that observed in $MnCr_2S_4$ crystals.[11] The suggestion of an antiferromagnetic order in the Mn sublattice in $MnCr_2S_4$ may then explain the observed value of saturation magnetization of about $6\mu_B$ found in high fields (~ 300 kOe),[9] when the magnetic moment of the Mn ions becomes perpendicular to the Cr moment. In this case the longitudinal component of the moment of the Mn ions becomes zero and only the Cr moment remains visible. From the entropy curve presented in the inset of Fig. 8(b) we can estimate the magnetic field which is necessary to result in a completely disordered Mn sublattice, i.e., the external field fully compensates the exchange field of the Cr sublattice. Extrapolation by the empirically found relation $S(T_{YK}) \sim H^{3/4}$ to a value $R \ln 6$ gives a value of a magnetic field of about 290 kOe. This value is in good agreement with the above mentioned saturation magnetic field and additionally supports the idea of antiferromagnetic ordering within the Mn sublattice.

With respect to the shift of the low-temperature λ anomaly (at T_{YK}) by an external magnetic field, we note that in pure antiferromagnets the application of a magnetic field usually shifts the transition temperature to lower temperatures.[46–48] In our case, due to the effect of the compensation of the exchange field of the Cr sublattice by the external magnetic field as discussed above, the Mn-Mn interactions result in an ordered state at higher temperatures and the magnetic field; thus, it has an opposite effect.

The role of the magnetocrystalline anisotropy is not clear yet. It may stabilize the low-temperature canted structure. In the case of $LaMnO_3$, e.g., the canting of the antiferromagnetic structure can only be understood by additional anisotropic interactions.[49] Considering the rather high value of the

anisotropy field H_A observed by us in $MnCr_2S_4$ single crystals [which is about one order of magnitude higher than that in the related spinel $CdCr_2S_4$ (Ref. 50)], it should be noted that the anisotropy cannot originate from the tetrahedrally coordinated Mn^{2+} ions or octahedrally coordinated Cr^{3+} ions because of the zero orbital momentum of the former and quenched orbital momentum of the latter ion in a cubic crystal field. The scaling between the first anisotropy constant K_1 and the normalized magnetization of the Cr sublattice $M_s/M_s(4\,\mathrm{K})$ as $K_1 \sim [M_s/M_s(4\,\mathrm{K})]^{10}$ agrees well with what is expected in the framework of a single-ion model.[27] This result indicates that the *B* sublattice is responsible for the anisotropic properties of $MnCr_2S_4$. The presence of a small amount of Mn^{3+} or Cr^{2+} ions on *B* sites caused by possible deviations from the stoichiometry could also be the reason of such an anisotropy. The relevance of the anisotropy for the low-temperature phase needs further experimental and theoretical investigation.

Although within our model it is possible to describe the observed peculiarities of magnetization and specific heat, a more complicated spin arrangement, e.g., a spiral configuration cannot be excluded for $MnCr_2S_4$. The Mn ions are arranged in two fcc sublattices, shifted against each other by (1/4, 1/4, 1/4) along the ⟨111⟩ direction. It is interesting to note that within the ideal cubic spinel structure the Mn-Mn exchange path, which consists of Mn-S-S-Mn chains, is the same within and between the respective Mn sublattices. This might prevent the formation of a simple collinear antiferromagnetic structure. The stability of a spiral arrangement in the spinels was theoretically established by Kaplan and others.[51,52] Experimentally, the helimagnetic type of ordering was found, for example, in the related $HgCr_2S_4$ and $MnCr_2O_4$ spinels.[53,54] It should be mentioned that recent experiments with triangular-lattice antiferromagnets have found strong variations of the temperature of the λ anomaly in the specific heat under application of a magnetic field.[55,56] For the helimagnetic configuration, an additional frustration, which appears in the triangular lattice, leads to a chiral degeneracy below the antiferromagnetic transition.[57] This question also needs further experimental study.

V. CONCLUSION

We have investigated the magnetization, ferromagnetic resonance, heat capacity, and conductivity in single crystals of the $MnCr_2S_4$ ferrimagnet. Pronounced λ anomalies in the heat capacity that accompany the magnetic phase transformations at the Curie temperature $T_C \sim 65$ K and at $T_{YK} \sim 4.8$ K were found. Both heat capacity anomalies are shifted to higher temperatures by the application of a magnetic field and correlate well with the behavior of the anomalies in the magnetization. The reduction of the magnetization below 42 K is accompanied by an entropy loss comparable to the full entropy change due to the ordering of the Mn sublattice. Ferromagnetic ordering of the Cr sublattice below T_C followed by quasiparamagnetic alignment of the Mn spins and final antiferromagnetic ordering within the Mn sublattice at T_{YK} is suggested to explain these observations. Magnetization and ferromagnetic resonance measurements revealed a strong magnetocrystalline anisotropy at low temperatures. A scaling of the first anisotropy constant K_1 with that of the tenth power of the magnetization of the *B* sublattice is found that indicates its dominating role in generating the magnetocrystalline anisotropy.

ACKNOWLEDGMENTS

This work was supported by Bundesministerium für Bildung und Forschung (BMBF) under Contract No. VDI/EKM 13N6917, Deutsche Forschungsgemeinschaft (DFG) via Contract No. SFB 484, and by U.S. Civilian Research & Development Foundation (CRDF) and Moldavian Research & Development Association (MRDA) via Grant No. MP2-3047.

[1] A. P. Ramirez, R. J. Cava, and J. Krajewski, Nature (London) **386**, 156 (1997).
[2] M. S. Park, S. K. Kwon, S. J. Youn, and B. I. Min, Phys. Rev. B **59**, 10 018 (1999).
[3] M. S. Park, S. K. Kwon, and B. I. Min, Phys. Rev. B **64**, 100403 (2001).
[4] F. K. Lotgering, Philips Res. Rep. **11**, 190 (1956).
[5] F. K. Lotgering, J. Phys. Chem. Solids **29**, 2193 (1968).
[6] N. Menyuk, K. Dwight, and A. Wold, J. Appl. Phys. **36**, 1088 (1965).
[7] V. Tsurkan, M. Demeter, B. Schneider, D. Hartmann, and M. Neumann, Solid State Commun. **114**, 149 (2000).
[8] J. Denis, Y. Allain, and R. Plumier, C. R. Seances Acad. Sci., Ser. B **269**, 740 (1969).
[9] J. Denis, Y. Allain, and R. Plumier, J. Appl. Phys. **41**, 1091 (1970).
[10] R. Plumier, R. Conte, J. Denis, and M. Nauciel-Bloch, J. Phys. (Paris), Colloq. **32**, C1-55 (1971).
[11] R. Plumier and M. Sougi, C. R. Seances Acad. Sci., Ser. B **268**, 1549 (1969).
[12] L. Néel, Ann. Phys. (Leipzig) **3**, 137 (1948).
[13] Y. Yafet and C. Kittel, Phys. Rev. **87**, 290 (1952).
[14] M. Nogues, M. Mejai, and L. Goldstein, J. Phys. Chem. Solids **40**, 375 (1979).
[15] R. Plumier, J. Phys. Chem. Solids **41**, 871 (1980).
[16] R. Plumier, C. R. Seances Acad. Sci., Ser. B **271**, 184 (1970).
[17] M. Nauciel-Bloch, A. Castets, and R. Plumier, Phys. Lett. A **39**, 311 (1972).
[18] V. Tsurkan, M. Mücksch, H.-A. Krug von Nidda, J. Hemberger, D. Samusi, A. Loidl, S. Horn, and R. Tidecks, Solid State Commun. **123**, 327 (2002).
[19] H. Schäfer, *Chemische Transportreaktionen* (Verlag Chemie, Weinheim, 1962).
[20] L. Darcy, P. K. Baltzer, and E. Lopatin, J. Appl. Phys. **39**, 898 (1968).
[21] R. P. Van Stapele, in *Ferromagnetic Materials*, edited by E. P.

Wohlfarth (North-Holland, Amsterdam, 1982), Vol. 3, p. 603.
[22] R. Bachmann, F. J. DiSalvo, T. H. Geballe, R. L. Greene, R. E. Howard, C. N. King, H. C. Kirsch, K. N. Lee, R. E. Schwall, H.-U. Thomas, and R. B. Zubeck, Rev. Sci. Instrum. **43**, 205 (1972).
[23] F. J. Morin and J. P. Maita, Phys. Rev. **129**, 1115 (1963).
[24] P. F. Sullivan and G. Seidel, Phys. Rev. **173**, 679 (1968).
[25] A. Arrott, J. Appl. Phys. **42**, 1282 (1971).
[26] M. Mejai and M. Nogues, J. Magn. Magn. Mater. **15–18**, 487 (1980).
[27] S. Chikazumi, *Physics of Ferromagnetism* (Clarendon, Oxford, 1997).
[28] The normalized $\tilde{K}_1(T)$ curve was adjusted at 7 K to the $[M_s(T)/M_s(4\,\mathrm{K})]^{10}$ curve for the Cr sublattice.
[29] S.-H. Lee, C. Broholm, T. H. Kim, W. Ratcliff II, and S.-W. Cheong, Phys. Rev. Lett. **84**, 3718 (2000).
[30] P. K. Baltzer, P. J. Wojtowicz, M. Robbins, and E. Lopatin, Phys. Rev. **151**, 367 (1966).
[31] V. K. Pecharsky, K. A. Gschneidner, Jr., and D. Fort, Phys. Rev. B **47**, 5063 (1993).
[32] P. Lin, S. H. Chun, M. B. Salamon, Y. Tomioka, and Y. Tokura, J. Appl. Phys. **87**, 5825 (2000).
[33] A. Cezairliyan and A. C. Anderson, *Specific Heat of Solids*, edited by C. Y. Ho (Hemisphere, New York, 1988).
[34] J. S. Kouvel, Phys. Rev. **102**, 1489 (1956).
[35] T. D. Edmons and R. G. Petersen, Phys. Rev. Lett. **2**, 499 (1959).
[36] S. S. Shinozaki, Phys. Rev. **122**, 388 (1961).
[37] S. R. Pollak and K. R. Atkins, Phys. Rev. **125**, 1248 (1962).
[38] V. Tsurkan, M. Baran, A. Szewczyk, R. Szymczak, and H. Szymczak, J. Phys.: Condens. Matter **11**, 7907 (1999).
[39] Y. X. Jia, Li Lu, K. Khazeni, D. Yen, C. S. Lee, and A. Zettl, Solid State Commun. **94**, 917 (1995).
[40] M. Viret, L. Ranno, and J. M. D. Coey, Phys. Rev. B **55**, 8067 (1997).
[41] A. Seeger, P. Lunkenheimer, J. Hemberger, A. A. Mukhin, V. Yu. Ivanov, A. M. Balbashov, and A. Loidl, J. Phys.: Condens. Matter **11**, 3273 (1999).
[42] V. Tsurkan, M. Baran, R. Szymczak, and H. Szymczak, J. Magn. Magn. Mater. **172**, 317 (1997).
[43] S. Pouget, M. Alba, and M. Nogues, J. Appl. Phys. **75**, 5826 (1994).
[44] C. I. Hsu, J. J. Steger, E. A. De Meo, A. Wold, and G. S. Heller, J. Solid State Chem. **13**, 304 (1975).
[45] B. Boucher, A. G. Herpin, and A. Oles, J. Appl. Phys. **37**, 960 (1966).
[46] W. L. Johnson and W. Reese, Phys. Rev. B **2**, 1355 (1970).
[47] J. H. Schelleng and S. A. Friedberg, Phys. Rev. **185**, 728 (1969).
[48] T. A. Reichert, R. A. Butera, and E. J. Schiller, Phys. Rev. B **1**, 4446 (1970).
[49] D. Ivannikov, M. Biberacher, H.-A. Krug von Nidda, A. Pimenov, A. Loidl, A. A. Mukhin, and A. M. Balbashov, Phys. Rev. B **65**, 214422 (2002).
[50] S. B. Berger and H. L. Pinch, J. Appl. Phys. **38**, 949 (1967).
[51] T. A. Kaplan, Phys. Rev. **119**, 1460 (1960).
[52] D. H. Lyons, T. A. Kaplan, K. Dwight, and N. Menyuk, Phys. Rev. **126**, 540 (1962).
[53] J. M. Hasting and L. M. Corliss, J. Phys. Chem. Solids **29**, 9 (1968).
[54] J. M. Hasting and L. M. Corliss, Phys. Rev. **126**, 556 (1962).
[55] H. A. Katori, K. Katsumata, and M. Katori, J. Appl. Phys. **81**, 4396 (1997).
[56] R. Bügel, J. Wosnitza, H. v. Löhneysen, T. Ono, and H. Tanaka, Phys. Rev. B **64**, 094406 (2001).
[57] H. Kawamura, J. Phys.: Condens. Matter **10**, 4707 (1998).